論文 Modeling Time-Dependent Response of Chloride-Induced Macrocell Corrosion of Steel in Concrete

Kai-Lin HSU[*1] and Tsuyoshi MARUYA[*1]

ABSTRACT: An integrated numerical procedure to trace time-dependent response of chloride-induced macrocell corrosion of steel in concrete by coupling the electrochemical models for the formation of natural potential and macrocell current density of being-corroded steel with the models dealing with the transport of the corrosion-induced mass is discussed in this paper. Furthermore, a few simulation results are illustrated to indicate the validity of this integrated numerical procedure.

KEYWORDS : macrocell corrosion, pit initiation, chloride threshold value, natural potential

1. INTRODUCTION

Due to the drastic development of experimental techniques, many physical or chemical phenomena related to concrete deterioration are being unfolded, which are generally recognized as the influencing factors of the long-term performance of concrete. On the other hand, due to the highly enhancement of computational ability of the digital computers, many researchers attempt to develop so-called life-span simulators of concrete from the elucidated knowledge relating to concrete deterioration. By avoiding introducing excessive empirical factors, the approaches based upon the microscopic modeling coupled with deterioration-related physio-chemical models [1,2] are prospective, which can be utilized to predict the distribution and accumulation of the deterioration factors in concrete. However, among the durability-related problems, corrosion of steel in concrete cannot be directly applied with the aforementioned techniques because corrosion of steel in concrete is known as an electrochemical process, which is out of the scope of the above physio-chemical models. For solving this task, the current approaches can be categorized into two types: the first one ,featured by treating the essence of corrosion mechanism as a black-box, is empirical-oriented by expressing the influence of significant corrosion factors in the form of functional relations [3] while the second one is to follow the known electrochemical processes and to characterize the corrosion rate of steel in the form of current density, which can be converted to corrosion rate of steel by Faraday's law [4,5]. Though complicated, the approaches categorized as the second type seem to arouse more researchers interest because not only the corrosion rate of steel but the other features of being-corroded steel (e.g. natural potential or polarization resistance, etc.) can be rationally modeled, which have been often adopted in assessing the corrosion behavior of steel in concrete.

In this research, the features of the electrochemical models for natural potential and macrocell current density of being-corroded steel due to chloride ingress are first described. Then, a numerical procedure is integrated by coupling the above models with the models dealing with the transport of the corrosion-induced mass earlier developed by the authors. Finally, the validity of this proposed procedure will be discussed by the illustration of some numerical examples.

[*1] Taisei Corporation, Technology Research Center

2. MODEL CONSTRUCTION

2.1 KINETICS OF REBAR CORROSION REACTIONS

For facilitating the following interpretation, a brief description on kinetics of corrosion reactions is given. As known, the high alkalinity of concrete (pH ≥ 12) protects the steel from corrosion due to the formation of passive film. However, due to low alkalinity and/or high chloride content at the surface of the steel, the passive film breaks down. Owing to the difference in potential between anode and cathode, iron is oxidized to ferrous ions at the anode and oxygen is reduced by releasing hydroxyl ions at cathode in accordance with

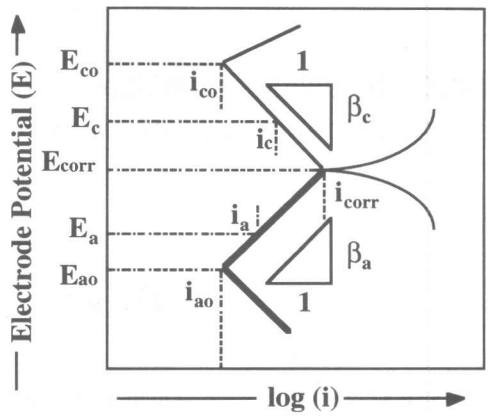

Fig.1 Polarization Model on Corrosion

Anode half-cell reaction :

$$Fe \Rightarrow Fe^{++} + 2e^- \quad (1.a)$$

Cathode half-cell reaction :

$$1/2O_2 + H_2O + 2e^- \Rightarrow 2OH^- \quad (1.b)$$

By assuming the polarization of each half-cell reaction as the simplified adaptation of Butler-Volmer kinetics, the relationship between potential and current density can be expressed as

Anode : $E_a = E_{ao} + \beta_a \log(i_a/i_{ao})$ (2.a) **Cathode :** $E_c = E_{co} + \beta_c \log(i_c/i_{co})$ (2.b)

where a and c : anode and cathode; E: potential; E_{xo} : equilibrium potential at x (i.e. a or c); β_x : activation Tafel slope for x; i_x : current density for x; i_{xo} : exchange current density for x. As schematized in **Fig.1**, the equilibrium potential for anode and cathode reactions is termed as corrosion potential (E_{corr}) and the correspondent current density at this potential is called corrosion current density (i_{corr}). Customarily, the measured corrosion potential of steel in concrete is often termed as natural potential because it can be also considered as the being-interacted state of the steel under natural environment.

2.2 MODEL FOR MICROCELL POTENTIAL OF CHLORIDE-INDUCED CORROSION

As observed, the chloride-induced rebar corrosion is in the form of pitting corrosion. Also, the pitting potential drops when pH in concrete falls and/or concentration of chloride gains; meanwhile, the natural potential also drops. By considering these features of natural potential of chloride-induced corrosion, a new model for microcell potential is proposed.

(a) pitting potential : by adopting the two-step initiation theory of pitting corrosion suggested by Okada [7], the pitting initiation potential (E_{pit}) was derived as

$$E_{pit} = -a \ln C_X + b \quad (3)$$

where $a = (qRT/\xi F)$: derived parameter; b is constant and C_X is the molar concentration of aggressive ion X at the surface of passive film. Besides, the linear relationship between the logarithmic of the activity of aggressive ions (e.g. Cl^-, Br^- or I^-) and the logarithmic of the activity of protective ions (e.g. OH^-, NO_3^- or SO_4^{2-}) is recognized [8], e.g.

$$\log a_{Cl^-} = c \log a_{OH^-} + d \quad (4)$$

where c and d are constants. Similar relation was reported in the work of Bird et al.[9] as

$$E_{pit} = -0.015 - 0.31 \log([Cl^-]/[OH^-]) \quad \text{(vs. SCE)} \quad (5)$$

Though the availability of Eq.(5) was originally applied in alkaline chloride solution rather than

in concrete, by considering the derivation process of Eqs. (3) and (4), the available expression for pitting initiation potential in concrete is expected to be similar to Eq.(5).

(b) chloride threshold value : according to the two-step initiation theory, the chloride threshold value can be considered as the minimum amount of chloride leading to pit initiation, which may follow the occurrence of perturbation , accumulation of chloride ion at the local anodic sites and the nuclei formation at the passive film surface. So far, the exact expression of chloride threshold value is still under argue. Here, the adopted expression is followed by the regression analysis on the results of the limited experiments carried by the authors as $[Cl^-]/[OH^-] = 4.7$. By comparing this empirical expression to the published data of the literature (e.g. **Table 1** in [10]), it is believed to be within acceptable scope.

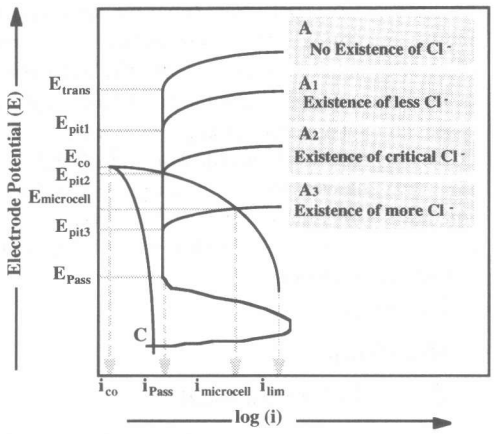

Fig.2 Model for Microcell Potential

(c) model for microcell potential : by observing the anodic and cathodic polarization curves as schematized in **Fig.2**, curve A depicts the case of no existence of Cl^-, under sufficient access of oxygen, the intersection of curve A and C (i.e. $E_{microcell}$,microcell potential) must be located between E_{trans} (transpassive potential) and E_{pass} (passive potential). With the increase of Cl^-, the correspondent E_{pit} (pitting potential) gradually drops. However, before reaching the threshold value of Cl^- (curve A_1), there is little influence from the drop of E_{pit} on the formation of $E_{microcell}$. On the other hand, once the chloride threshold value is exceeded, $E_{microcell}$ will be more lower than the correspondent E_{pit}. In other words, if E_{pit} is lower than the cathodic potential (E_c) at passive current density (i_{pass}), the pitting corrosion is initiated. Based on these understandings, the algorithm to calculate $E_{microcell}$ is introduced as follows:

Step 1. E_c at i_{pass} can be calculated from pH and the concentration of O_2 at the surface of passive film, by applying Nernst Equation for cathodic reaction as well as Eq.(2.b).

Step 2. E_{pit} can be calculated from pH and the concentration of Cl^- at the surface of passive film, by applying Eq.(5) if the chloride threshold value is exceeded. If not exceeded, $E_{pit} = E_{trans}$.

Step 3. By comparing the calculated E_c with the calculated E_{pit}, if $E_c < E_{pit}$, there is no pitting corrosion (i.e. $E_{microcell} = E_c$) while , if $E_c > E_{pit}$, pitting corrosion is judged to occur so that $E_{microcell}$ can be calculated by applying Nernst Equation for anodic reaction as well as Eq.(2.a). Also, the correspondent microcell current density ($i_{microcell}$) can be calculated.

2.3 MODEL FOR MACROCELL CURRENT DENSITY

In the previous section, the algorithm to calculate $E_{microcell}$ of chloride-induced rebar corrosion is illustrated. The term "microcell" is adopted for the assumption that the formation of the polarized potential at separate electrode (i.e. the point at the surface of rebar) is independent without the interaction between separate electrodes. If no pitting corrosion, the microcell potential can be regarded as the measured natural potential at its passive state. However, once pitting corrosion is initiated, macrocell current is notorious for its flow between the anodes and cathodes, which causes lots of damage to RC structures. Here, by assuming there exists the interaction between the separate electrodes after the formation of microcell potential of separate electrodes, a new model used for the formation of the macrocell current density at separate electrodes is proposed.

(a) activation polarization : according to the assumption used in the previous section, after the formation of microcell potential , the state of separate electrodes should be regarded as stable due

no interaction between separate electrodes. However, once the interaction between electrodes is taken into account, the activation polarization is indispensable for generating the essential activation energy needed in the corrosion reactions. As illustrated in **Fig.3**, for any two electrodes, if pitting corrosion is initiated, the macrocell current density (i_{corr}) can be calculated by solving the following nonlinear equation :

$$E_{ma,c} - E_{ma,a} = (L_{ac}\, w)\, i_{corr} = (E_{mi,c} + \beta_{c1}\, log\, (i_{corr}/i_{mi,c})) - (E_{mi,a} + \beta_{a2}\, log\, (i_{corr}/i_{mi,a})) \quad (6)$$

where L_{ac} : distance bwteen anode and cathode (cm); W : concrete resistivity (Ω-cm) .

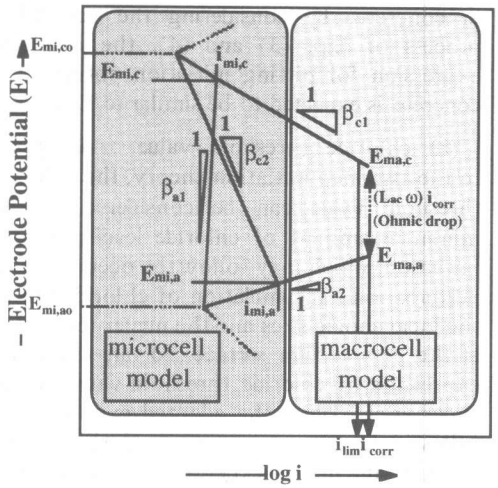

Fig.3 Model for Macrocell Current Density

For β_a and β_c, the empirical expressions in [6] (ref. to Eqs.(6.1.10) and (6.1.11)) are adopted for the compatibility on RC structures. Method of False Position is used for the solution of the above nonlinear equation. For anode, the value of i_{corr} takes negative to indicate the inflow of current while, for cathode, that of i_{corr} takes positive to indicate the outflow of current.

(b) limiting current density : due to the cover thickness of concrete, saturation degree of concrete and environmental conditions, etc., the access of O_2 at the surface of passive film may be insufficient, which renders corrosion reaction diffusion-limited. By referring to Eqs.(6.1.5) and (6.1.6) in [6], the limiting current density of O_2 (i_{lim}) can be calculated.

(c) model for macrocell current density : as mentioned, the model schematized in **Fig.3** is valid for any two electrodes once pitting corrosion is initiated. However, as known, there are usually lots of electrodes distributed along any rebar. That is to say, for any electrode, there should exist multiple electrical circuits. For solving this task, the steps below are taken:

Step 1. for N electrodes along the rebar, the number of the possible electrical circuits is 1/2N(N-1).By applying Eq.(6) for all the possible electrical circuits, the anodic and cathodic current density for each circuit can be obtained.

Step 2. by applying principle of superposition at each electrode, the net macrocell current density at each electrode can be calculated.

Step 3. By the sign of the net macrocell current density , the correspondent electrode can be judged as anode (if sign < 0) or cathode (if sign > 0). For the electrodes as cathode, by comparing the calculated i_{lim} with the calculated i_{corr}, if $i_{lim} \geq i_{corr}$, the calculated i_{corr} needs no modification while , if $i_{lim} < i_{corr}$, the following modification is needed : first, by introducing the condition that the value of inflow and outflow current be equal, the excessive current density at cathode (i.e. $i_{corr} - i_{lim}$)divided by the number of possible circuits is subtracted from the current density at each anode.

(d) macrocell (natural) potential : as can be observed in **Fig.3**, the microcell potential at separate electrode is polarized due to the activation and/or concentration (i.e. diffusion-limited) polarization. Through the above modeling, the possibility of owing different amount of polarization for an electrode, due to the existence of multiple electric circuits, contradicts the reality of the measured natural potential of rebar. Because ,up to now, there is little research reported on how the process of being-polarized rebar is, the averaged amount of polarization for an electrode is used for its simplicity. Then, the distribution of macrocell (natural) potential along rebar can be calculated.

Table 1 Case for Analytical Conditions

Case	T_{dry} (days)	T_{wet} (day)	T_{cyc} (days)	c (cm)	d (cm)
101cd22	100	1	101	2	2
101cd62	100	1	101	6	2
101cd66	100	1	101	6	6
11cd22	10	1	11	2	2
11cd62	10	1	11	6	2
11cd66	10	1	11	6	6

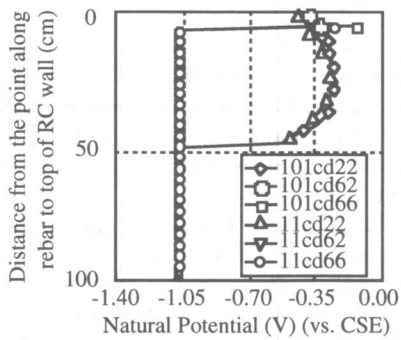

Fig.5 Comparison on Natural Potential

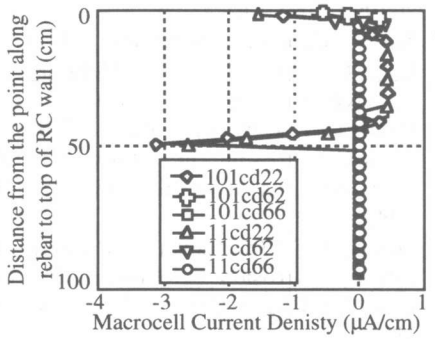

Fig. 6 Comparison on Macrocell Current Density

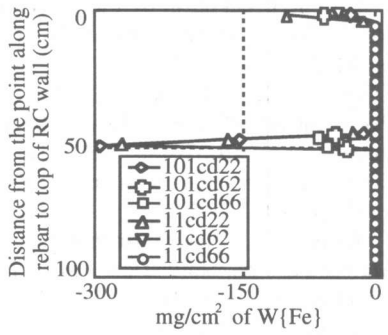

Fig.7 Comparison on Corroded Amount of Fe

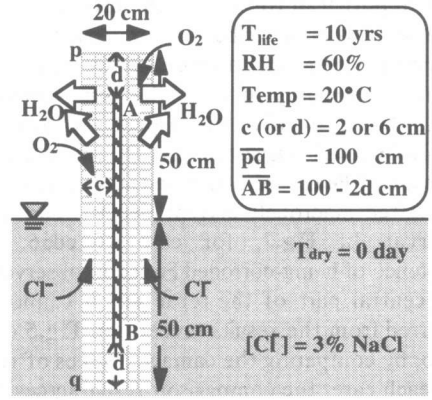

Fig.4 Layout of Marine RC Wall

3. RESULTS AND DISCUSSION

In order to verify the proposed models, an integrated numerical procedure was implemented by coupling them with the models dealing with the transport of the corrosion-induced mass, which were earlier developed by the authors [2]. To evaluate the validity of this integrated numerical procedure, the case for the simulation of the life-span of the marine RC wall exposed under various cyclic drying-wetting conditions is used. The simulation period is considered as 10 yr. The mixing proportion of concrete can be referred to **Table 9.2** in [11]. In addition, the diffusion coefficient used for the calculation of moisture and chloride are 12.0~2.04 and 1.37~1.64 (x $10^{-3}cm^2$/day) respectively. The layout of the specimen is shown in **Fig.4**. The cyclic drying-wetting interval (T_{cyc}) is composed of dry interval (T_{dry}) and wet interval (T_{wet}). These analytical conditions are labeled in **Table 1**. With these conditions, the simulated results are given in **Figs.5-8**. In **Fig.5**, as can be referred to point C in **Fig.2**, the natural potential of the submerged part or the part with little concentration of O_2 is kept under -1000 mV (vs. CSE) because the insufficient supply of O_2. On the other hand, although the distribution of natural potential implies the existence of the being-corroded parts, it is difficult to judge the exact location of being-corroded parts, This task can be solved by referring to **Fig.6**, which distinguishes the location of the anodes and cathodes along the rebar. However, under cyclic drying-wetting condition, the distribution of

natural potential (or macrocell current density) cannot always describe the existence of the corrosion product because there may be insufficient supply of O_2 at the being-corroded parts. For explaining this aspect, by referring to Eq.(6.2.32) suggested in [6], the corroded amount of Fe can be converted according to the calculated macrocell current density and time interval. In **Fig.7**, for case 101cd66, the existence of being-corroded Fe can be observed at the central part of the rebar which cannot be inferred from the results revealed in **Fig.5** or **6**. Also, by comparing the damage degrees of rebar for each case, the comparison result agrees well with the expected results on these cases. Next, by taking the derivative of corroded amount of Fe with respect to time at the central point along rebar , the corrosion rate of Fe can be obtained as shown in **Fig.8** , which indicates case 101cd66 starts to corrode roughly after 4th year. This confirms the observation for case 101cd66 in **Fig.7**. In addition, the corrosion rate of Fe for the most damaged cases seems to decrease after a certain period, which can be considered as the decrease of the potential difference between nodes due to the gradual closeness of $[Cl^-]$ at each node.

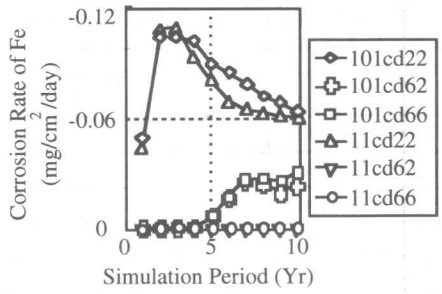

Fig.8 Comparison on Corrosion Rate of Fe

4. CONCLUDING REMARKS

Through the examples for verification, the validity of the proposed models on tracing time-dependent response of chloride-induced macrocell corrosion of steel in concrete could be considered to be accepted because the simulated results on the example structure rationally reflect the behavior of life-time state of the example structure during their simulation period.

REFERENCES

[1] Maekawa, K., Chaube,R.P., and Kishi,T.,"Coupled Mass Transport, Hydration and Structure Formation Theory for Durability Design of Concrete Structures", Proc. Intn'l Workshop on Rational Design of Concrete Structures Under Sever Conditions, Hakodate,1995, pp.263-274.

[2] Maruya, T. and Hsu, K.L., "Numerical Simulation on Cl^-, Moisture, O_2 and CO_2 in Concrete", 42th Proc. of Japan Congress on Materials Research, Sep. 1998, pp.132-133.

[3] Zivica, V., "The Rate of Corrosion of Concrete Reinforcement and Possibilities of its Mathematical Modelling", Bull. Mater. .Sci.,Vol.18,No.2,Apr. 1995, pp.115-124.

[4] Uhlig, H.H. , Corrosion and Corrosion Control, second ed., 1971.

[5] Kranc, S.C. and Sagues, A.A., "Computation of Reinforcing Steel Corrosion Distribution in Concrete Marine Bridge Substructures",Corrosion,Vol.50,No .1,1994, pp.50-61.

[6] Japan Concrete Instituite, Technical Report on Repair Methods of Concrete Structures (III), 1996.

[7] Okada, T., "Two-step Initiation Theory of Pitting Corrosion in Passive Metals", Boshoku Gijutsu,Vol.36, 1987, pp.787-794.

[8] Okada, T., "Breakdown of Passivity and Pitting Corrosion - Kinetic Process", Boshoku Gijutsu,Vol.36, 1987, pp.383-392.

[9] Bird, H.E.H., Pearson, B.R. and Brook, P.A.,"The Breakdown of Passive Films on Iron", Corrosion Sci., Vol.28, No.1,1988, pp.81-86.

[10] Glass, G.K. and Buenfeld, N.R., "The Presentation of the Chloride Threshold Level for Corrosion of Steel in Concrete",Corrosion Science,Vol.39,No.5, 1997, pp.1001-1013.

[11] Maruya, T., Tangtermsirikul, S. and Matsuoka, Y.,"Simulation of Chloride Penetration into Hardened Concrete", Durability of Concrete, ACI SP-145, pp.519-538,1994.